

**Observed temporal
evolution of global
age of air**

G. P. Stiller et al.

Observed temporal evolution of global mean age of stratospheric air for the 2002 to 2010 period

G. P. Stiller¹, T. von Clarmann¹, F. Haenel¹, B. Funke², N. Glatthor¹,
U. Grabowski¹, S. Kellmann¹, M. Kiefer¹, A. Linden¹, S. Lossow¹, and
M. López-Puertas²

¹Karlsruhe Institute of Technology, Institute for Meteorology and Climate Research, Karlsruhe, Germany

²Instituto de Astrofísica des Andalucía, CSIC, Granada, Spain

Received: 28 July 2011 – Accepted: 7 October 2011 – Published: 18 October 2011

Correspondence to: G. P. Stiller (gabriele.stiller@kit.edu)

Published by Copernicus Publications on behalf of the European Geosciences Union.

Title Page

Abstract

Introduction

Conclusions

References

Tables

Figures

◀

▶

◀

▶

Back

Close

Full Screen / Esc

Printer-friendly Version

Interactive Discussion



Abstract

An extensive observational data set, consisting of more than 10^6 SF₆ vertical profiles distributed globally from MIPAS measurements has been condensed into monthly zonal means of mean age of air for the period September 2002 to January 2010, binned at 10° latitude and 1–2 km altitude. The data were analysed with respect to their temporal variation by fitting a regression model consisting of a constant and a linear increase term, 2 proxies for the QBO variation, sinusoidal terms for the seasonal and semi-annual variation and overtones for the correction of the shapes to the observed data set. The impact of subsidence of mesospheric SF₆-depleted air and in-mixing into non-polar latitudes on mid-latitudinal absolute age of air and its linear increase was assessed and found to be small.

The linear increase of mean age of stratospheric air was found to be positive and partly larger than the trend derived by Engel et al. (2009) for most of the Northern mid-latitudes, the middle stratosphere in the tropics, and parts of the Southern mid-latitudes, as well as for the Southern polar upper stratosphere. Multi-year decrease of age of air was found for the lowermost and the upper stratospheric tropics, for parts of Southern mid-latitudes, and for the Northern polar regions. Analysis of the amplitudes and phases of the seasonal variation shed light on the coupling of stratospheric regions to each other. In particular, the Northern mid-latitude stratosphere is well coupled to the tropics, while the Northern lowermost mid-latitudinal stratosphere is decoupled, confirming the separation of the shallow branch of the Brewer-Dobson circulation from the deep branch. We suggest an overall increased tropical upwelling, together with weakening of mixing barriers, especially in the Northern Hemisphere, as a hypothetical model to explain the observed pattern of linear multi-year increase/decrease, and amplitudes and phase shifts of the seasonal variation.

ACPD

11, 28013–28059, 2011

Observed temporal evolution of global age of air

G. P. Stiller et al.

Title Page

Abstract

Introduction

Conclusions

References

Tables

Figures

◀

▶

◀

▶

Back

Close

Full Screen / Esc

Printer-friendly Version

Interactive Discussion



1 Introduction

The increase of greenhouse gas abundances in the atmosphere is associated with an increased radiative forcing, leading to a warming of the troposphere and a cooling of the stratosphere (IPCC, 2007). A secondary effect of increasing levels of greenhouse gases is a possible change in the stratospheric circulation (Butchart et al., 2006) with substantial feed-backs on chlorofluorocarbon lifetimes (Butchart and Scaife, 2001; Douglass et al., 2008), ozone (Shepherd, 2008) and the climate system (Baldwin et al., 2007). Model calculations (Waugh and Hall, 2002) have shown that the mean age of air in the stratosphere is a good indicator of the strength of the residual circulation (Li and Waugh, 1999) and that mean age is expected to decrease (Austin et al., 2007; Austin and Li, 2006; Garcia and Randel, 2008; McLandress and Shepherd, 2009; Oman et al., 2009; SPARC CCMVal, 2010). An increase in the rate of up-welling in the tropical lower stratosphere is predicted by all atmospheric general circulation models (Butchart et al., 2006) and is consistent with the observed long term temperature decrease in the tropical tropopause region (Thompson and Solomon, 2005). The models indicate that a change in the mean age of air has occurred over the past 40 yr, with a decrease of mean age mainly occurring after 1975, coupled to an increase in mean tropical up-welling. Most models derive a decrease in the range of -0.20 to -0.05 yr decade⁻¹ (Waugh, 2009).

Based on meteorological data, positive anomalies in tropical upwelling have also been derived for the period from 2001 to 2004 when compared to the long term mean (Randel et al., 2006). An extended study using tropical ozone data from SAGE II and the SHADOZ ozonesonde network for the years 1984 to 2009 detected negative ozone trends consistent to systematic increases in tropical stratospheric upwelling (Randel and Thompson, 2011). A drop in tropical lower stratospheric water vapor in the year 2000 with persistently lower values in the following years has also been linked to colder tropopause temperatures due to increased tropical upwelling (Rosenlof and Reid, 2008; Solomon et al., 2010; Dhomse et al., 2008). If this increased upwelling

Observed temporal evolution of global age of air

G. P. Stiller et al.

Title Page

Abstract

Introduction

Conclusions

References

Tables

Figures



Back

Close

Full Screen / Esc

Printer-friendly Version

Interactive Discussion



also leads to an increase in the overall residual circulation of the stratosphere (Brewer-Dobson circulation), then shorter transport times and shorter residence times of some greenhouse gases and ozone-depleting substances (ODS) are expected, as these are mainly photolysed at altitudes above 20 km in tropics, leading to decreased atmospheric lifetimes. An increased upwelling which is restricted to the lowest part of the tropical stratosphere, however, would have a much smaller feed-back on the lifetimes of ODSs.

The studies above indicate that a change in the mean circulation may occur, which could lead to changes in mean age and may have a strong impact on the overall composition of the stratosphere. The mean age may be the most suitable tracer to detect such changes in atmospheric coupling. As the expected changes in mean age are reported to be in the order of 10 to 20 % only (Austin and Li, 2006), they are difficult to detect from observations, which are influenced by atmospheric variability and by systematic errors in the derivation of mean age.

Mean age can be derived from observations of tracers which increase with time in the atmosphere and show neither sinks nor sources in the middle atmosphere. The two tracers that have been used most widely to derive mean age are carbon dioxide (CO_2) and sulfur hexafluoride (SF_6). Both of these tracers have somewhat different characteristics: CO_2 has a seasonal cycle in the troposphere which can propagate into the stratosphere and makes the determination of mean age values below 2 yr ambiguous. It also has a stratospheric source due to the oxidation of methane and the reaction $\text{CO} + \text{OH}$, which can however be corrected for if methane is measured simultaneously. Furthermore, the growth rate of CO_2 shows considerable interannual variability, as it is strongly coupled to the biosphere. Such interannual variability may lead to systematic uncertainties in the dating of the air. SF_6 , on the other hand, increases monotonically and with small interannual variability in the troposphere but has a sink in the mesosphere, which can cause an artefact when dating old air (Waugh and Hall, 2002; Strunk et al., 2000; Reddmann et al., 2001; Engel et al., 2002; Ray et al., 2002; Plumb et al., 2002; Engel et al., 2006; Stiller et al., 2008).

Observed temporal evolution of global age of air

G. P. Stiller et al.

Title Page

Abstract

Introduction

Conclusions

References

Tables

Figures

◀

▶

◀

▶

Back

Close

Full Screen / Esc

Printer-friendly Version

Interactive Discussion



The only long-term observational data set on age of air available so far, provided by Engel et al. (2009), however, did not confirm model results predicting the decrease in age of air. The authors derived an increase of $+0.24 \pm 0.22$ ($1-\sigma$) yr decade^{-1} for Northern mid-latitudes over the period of 1975 to 2005, which is inconsistent to the upper limit of the model predictions ($-0.25 \text{ yr decade}^{-1}$) on a confidence level of 95 %, while the lower end of the predictions ($-0.08 \text{ yr per decade}$) could not be falsified on the 95 % confidence level.

Recent publications (e.g. Garcia et al., 2011) argue that a data set as sparse as the Engel et al. (2009) time series was not useful for estimating a decadal trend, supporting this statement with similar sampling exercises on their model results. These authors emphasize the need for well-sampled observations of strictly linearly growing tracers which, as they say, are not available.

In this paper, we present observations of SF_6 by the MIPAS satellite instrument from which stratospheric mean age of air is derived. Section 2 describes the measurements and the retrieval procedure to derive SF_6 . In Sect. 3, the derivation of mean age of stratospheric air from the observed global fields of SF_6 is described, and global distributions of mean age of air will be presented. The methods of quantitative analysis of the temporal development of monthly zonal mean age of air, based on a 10° -latitude times 1–2 km altitude gridding of all data, and covering the period September 2002 to January 2010, will be presented in Sect. 4. In Sect. 5, these methods are applied to MIPAS age of air data for analysis of seasonal and long-term variation for each latitude and altitude. The impact of model errors and data autocorrelation is assessed in Sect. 7. In Sect. 8 we summarise the results in the light of possible changes of the Brewer-Dobson circulation.

2 MIPAS measurements and data

The Michelson Interferometer for Passive Atmospheric Sounding (MIPAS) is a Fourier-Transform Infrared Spectrometer with high spectral resolution which was launched into a sun-synchronous orbit aboard the Environmental Satellite (Envisat) on

Observed temporal evolution of global age of air

G. P. Stiller et al.

Title Page

Abstract

Introduction

Conclusions

References

Tables

Figures

◀

▶

◀

▶

Back

Close

Full Screen / Esc

Printer-friendly Version

Interactive Discussion



1 March 2002. From 2002 to March 2004 it provided about 1000 limb sequences of mid-infrared radiance spectra per day along 14.4 orbits in the 4.15 to 14.6 μm range with a spectral resolution of 0.035 cm^{-1} , a vertical sampling of 3 km in the upper troposphere and stratosphere range, and a horizontal sampling of 510 km along-track (Fischer et al., 2008). The instantaneous field of view covers 3 km in the vertical and 30 km in the horizontal direction. After a problem with the interferometer slide which caused an interruption of operation, MIPAS resumed measurements in January 2005 with slightly degraded spectral (0.0625 cm^{-1}), but improved spatial resolution (vertical sampling 1.5 km up to 22 km, increasing to 3 km in the upper stratosphere, sampling along-track between 275 and 410 km depending on observation mode).

Vertical profiles of SF_6 were retrieved from the measurements of the first operation period (September 2002 to March 2004, ESA data version 4.61/4.62) from the spectral signature near 948 cm^{-1} as described by Stiller et al. (2008). The slightly degraded spectral resolution of the MIPAS operation mode since January 2005 (ESA data version 4.67) required some adjustment of the retrieval set-up. An extended spectral range from 941.0 to 952.0 cm^{-1} was used for the retrieval in order to have more independent information on lines of other species at the reduced spectral resolution. The improved vertical sampling, however, allowed for a relaxation of the vertical regularization within the Tikhonov-constrained global-fit approach (Tikhonov, 1963; Steck and von Clarmann, 2001). Radiance measurements up to 41 km tangent altitude were used within the retrieval.

The adjusted retrieval set-up resulted in vertical profiles of SF_6 covering the 6 to 40 km altitude range with typical measurement noise errors of 10 to 20 % (single scan). The total precision, including all randomly varying parameter errors has remained similar to observations of the first MIPAS mission period and is estimated at 10 to 40 % (single scan) (Stiller et al., 2008). For comparison, the standard deviation (standard error) of the daily zonal mean covering a 5° latitude bin is in the range of 8 to 16 % (1 to 2 %), including both the total precision of the measurements and the natural variability within the latitude band.

Observed temporal evolution of global age of air

G. P. Stiller et al.

Title Page

Abstract

Introduction

Conclusions

References

Tables

Figures

◀

▶

◀

▶

Back

Close

Full Screen / Esc

Printer-friendly Version

Interactive Discussion



Observed temporal evolution of global age of air

G. P. Stiller et al.

Title Page

Abstract

Introduction

Conclusions

References

Tables

Figures

◀

▶

◀

▶

Back

Close

Full Screen / Esc

Printer-friendly Version

Interactive Discussion



Systematic errors not varying in sign with time and thus potentially contributing to a systematic bias were estimated at about 6 % (Stiller et al., 2008), resulting in a total accuracy of a single profile (summing up all random and systematic errors according to Gaussian error propagation) of 12 to 40 %. The vertical resolution of the profiles is 4 km (up to 20 km altitude) to 6 km (at 30 km altitude), increasing to 8 km at 40 km and above. MIPAS SF₆ profiles have been validated versus measurements of a balloon-borne cryogenic whole-air sampler (Engel et al., 2006), and agreement within 0.5 pptv has been found for close coincidences and similar air masses (in terms of potential vorticity) sampled (Stiller et al., 2008).

For more details on the retrieval procedure and the estimation of random and systematic errors we refer to Stiller et al. (2008). The calibration insufficiency reported there was not present in ESA version 4.67 spectral data provided since January 2005. Thus, the correction scheme described in Stiller et al. (2008) needed not to be applied to SF₆ profiles measured in the years 2005 to 2010. Spectral data from both the nominal observation mode (covering 6 to 70 km, NOM) and the UTLS observation mode (covering 5.5 to 50 km) have been used, and the same retrieval set-up could be applied, since for altitudes relevant to this paper both observation modes are equivalent. Figure 1 provides the time series of SF₆ volume mixing ratio over all latitudes at 25 km altitude. The continuous growth of SF₆ at all latitudes, but also seasonal and other temporal variations are clearly seen. Over all, more than 10⁶ retrieved profiles of SF₆ covering the period September 2002 to end of January 2010, have been combined to the data set analysed further in this paper.

3 Tropical tropospheric increase of SF₆ and conversion into age of air

The age of stratospheric air is derived from a stable tracer of a monotonically increasing mixing ratio by comparison of its actual stratospheric mixing ratio with a time series of tropospheric mixing ratios. The time lag between the date of the stratospheric measurement and the time when the same mixing ratio was measured in the troposphere is

the age of air. For this analysis, the comparability of tropospheric data and the MIPAS measurements has been tested (Sect. 3.1), and a tropospheric reference curve reflecting the SF₆ increase with time was constructed (Sect. 3.2). Mixing of stratospheric air along with a nonlinear reference curve requires a correction (Sect. 3.3), before reliable age of air distributions can be presented (Sect. 3.4).

3.1 Comparison of tropical free troposphere data to ground-based in situ data

Daily mean mixing ratios of SF₆ in the region of the upper tropical troposphere within 9 to 15 km altitude and from 17.5° S to 17.5° N as function of time were derived from MIPAS observations and compared both to SF₆ global monthly means from the National Oceanic and Atmospheric Administration, Earth System Research Laboratory (NOAA/ESRL) halocarbons program retrieved from ftp://ftp.cmdl.noaa.gov/hats/sf6/combined/HATS_global_SF6.txt. The data set from NOAA/ESRL is a combination from two measurement programs. Weighted averages of monthly mean data are combined, interpolated, and smoothed for each sampling location. Hemispheric and global means are estimated by cosine weighting by latitude (see Hall et al. (2011) for more details). Further, MIPAS data were compared to in situ ground-based observations in the tropics (Mauna Loa Observatory and American Samoa) (Elkins and Dutton, 2009; Rigby et al., 2010; Hall et al., 2011) (see Fig. 2, top panel). The MIPAS SF₆ volume mixing ratios from the upper tropical troposphere compare well with both the in situ ground-based tropical data and the combined flask/in situ global means. In particular, the temporal evolutions of all data sets demonstrate that, as already reported by Levin et al. (2010), Rigby et al. (2010), and Hall et al. (2011), tropospheric SF₆ volume mixing ratios have started to grow clearly stronger than linear in 2006, with continuously increasing growth rates until 2009. A closer look to the consistency of all data sets is provided in Fig. 2, lower panels. The daily mean deviations between MIPAS tropical upper tropospheric SF₆ vmr and the three combined or in situ data sets reveal that:

Observed temporal evolution of global age of air

G. P. Stiller et al.

Title Page

Abstract

Introduction

Conclusions

References

Tables

Figures

◀

▶

◀

▶

Back

Close

Full Screen / Esc

Printer-friendly Version

Interactive Discussion



- i. a bias of (-0.111 ± 0.013) pptv exists between the MIPAS 2002–2004 and 2005–2010 data sets (2005 to 2010 period being lower), determined consistently from all three combined or in situ observational data sets;
- ii. the MIPAS 2002 to 2004 data set agrees best with the combined global mean data, with a bias of only -0.013 pptv;
- iii. MIPAS SF₆ is lower than the Mauna Loa Observatory data which represent the Northern Hemisphere tropics (19.539° N, 155.578° W, elevation: 3397 m), and higher than the American Samoa data which represent the Southern Hemisphere tropics (14.3° S, 170.6° W, elevation: 77 m), reflecting the bias between Northern and Southern Hemisphere due to the transport barrier.

All in all MIPAS tropical upper troposphere SF₆ vmr can be considered representative for the tropics; any difference between the ground-based data and the upper troposphere MIPAS data is below or, at most, similar to the accuracy of the MIPAS daily mean data; further, with transport times of hours to days from the ground to the free upper troposphere we do not expect any significant delay of upper tropospheric SF₆ vmrs compared to the values at the ground. For all data used in the following work, the bias between the 2002–2004 and 2005–2010 MIPAS data set has been corrected for by increasing all 2005 to 2010 data by 0.111 pptv at all altitudes and latitudes. This is probably an oversimplified approach, but the best we can do at that time.

3.2 Reference curve

For calculation of mean age of air from observed SF₆ distributions in the stratosphere, we need reference SF₆ abundances at the entry point to the stratosphere, i.e. the tropical tropopause region. We have constructed a SF₆ reference curve from independent observations from the NOAA/ESRL data sets: for the period 1996 to May 2011 we used a smoothed time series of monthly global mean combined flask and in situ data as described in Hall et al. (2011) (smoothed by an 11-months running mean, violet solid

Observed temporal evolution of global age of air

G. P. Stiller et al.

Title Page

Abstract

Introduction

Conclusions

References

Tables

Figures

⏪

⏩

◀

▶

Back

Close

Full Screen / Esc

Printer-friendly Version

Interactive Discussion



line in Fig. 2, widely overlaid by the orange curve), while for the period 1987 to 1996 we used the linear approximation $y = 0.125 + 0.215 \times (t - 1985)$ as provided by Hall et al. (2011). Since MIPAS measurement uncertainties may lead to SF₆ volume mixing ratios slightly larger than the highest abundances in the reference data set, which will result in negative age of air values, an extension to data beyond January 2010 was necessary. We have used a linear extrapolation with the averaged slope of the last year of the NOAA/ESRL data for this purpose. The reference curve is shown as orange line in Fig. 2.

3.3 Non-linearity correction

If the tropospheric trend of SF₆ was exactly linear, the determination of the mean age of stratospheric air would be an almost trivial task: The linear regression function representing the tropospheric mixing ratio as a function of time could easily be inverted and the age of the sounded air parcel could be calculated as the time lag Δt between the date of the measurement t and the date in the past t' when the measured mixing ratio was found in the troposphere. Even the fact that the sounded air parcel had been subject to mixing processes would not cause major difficulties because, due to the linear relationship between tropospheric SF₆ mixing ratio and time, the measured mixing ratio in an air parcel would still represent the mean age of air, regardless what the age distribution within the air parcel might be (e.g. Waugh and Hall, 2002). Unfortunately, the tropospheric mixing ratio of SF₆ is a slightly nonlinear function of time, and a more sophisticated approach is needed. In agreement with literature (e.g. Andrews et al., 1999) we describe the age spectrum by a Green's function G . As shown in several studies (Waugh and Hall, 2002), the Green's function of a one-dimensional model can already approximate the Green's function of the real stratosphere quite well. This particular Green's function can be represented by a Wald (inverse Gaussian) function

Observed temporal evolution of global age of air

G. P. Stiller et al.

Title Page

Abstract

Introduction

Conclusions

References

Tables

Figures

◀

▶

◀

▶

Back

Close

Full Screen / Esc

Printer-friendly Version

Interactive Discussion



$$G(\Gamma, \Delta, t') = \frac{1}{2\Delta\sqrt{\pi t'^3}} \exp\left[\frac{-\Gamma^2(t' - 1)^2}{4\Delta^2 t'}\right] \quad (1)$$

with Γ being the mean age of stratospheric air, $t' = \Delta t/\Gamma$, Δt the transit time of an air parcel from the stratospheric entry point at the tropical tropopause to the relevant location in the stratosphere, and Δ being the width of the distribution. For Δ we use the approximation according to Waugh and Hall (2002)

$$w = \Delta^2/\Gamma = \text{constant} \approx 0.7. \quad (2)$$

In a first step of our iterative approach we determine a first guess of the age of the air parcel by simply mapping the measured SF_6 mixing ratio onto the time axis. For this initially guessed age we determine the width Δ of the age spectrum using the relation in Eq. 2 and apply the spectrum to the tropospheric SF_6 -time relationship (Fig. 2, top panel) to give the $[\text{SF}_6]_{\text{modeled}}$, which is the SF_6 mixing ratio which would correspond to the initially guessed age of the sounded air parcel:

$$[\text{SF}_6]_{\text{modeled}} = \int_t G(\Gamma, \Delta, t) \cdot [\text{SF}_6]_{\text{trop}}(t) dt \quad (3)$$

The residual $[\text{SF}_6]_{\text{modeled}} - [\text{SF}_6]_{\text{measured}}$ and the inverse first derivative $(d[\text{SF}_6]_{\text{trop}}/dt)^{-1}$ of the tropospheric SF_6 -time relationship allow to determine the actual mean age of the measured air parcel by Newtonian iteration. The correction is not strictly monotonically increasing with age due to the variations in the SF_6 reference curve (smoothed combined flask and in situ observations). The difference of the initially guessed age and the final result, i.e. the effect of the age spectrum and the nonlinearity of the tropospheric SF_6 -time relationship ranges from -0.1 to 0.2 yr for ages between 0 and 10 yr, and up to 0.8 yr for ages higher than 10 yr. This is in good agreement to results derived by Volk et al. (1997), who assessed the necessary correction of age of air calculation for the case of quadratic increase. Although a correction of up to 0.8 years seems to be considerable, almost nothing changed at the

Observed temporal evolution of global age of air

G. P. Stiller et al.

Title Page

Abstract

Introduction

Conclusions

References

Tables

Figures

◀

▶

◀

▶

Back

Close

Full Screen / Esc

Printer-friendly Version

Interactive Discussion



relative patterns and variations of global age of air distributions as presented in the next Section.

The assumption that the width of the age spectrum Δ is given by $w = \Delta^2 / \Gamma = \text{const.} \approx 0.7$ which has been used in the correction procedure described above does certainly not strictly hold for all altitude/latitude regions of the stratosphere. On the other hand, little is known on realistic age spectra and their variation from observations (cf. Schoeberl et al., 2005), so that $w = 0.7$ seems to be an acceptable approximation for the moment. Model assessments result in a variation of w between 0.4 and 1.5 yr (Hall and Plumb, 1994; Waugh et al., 1997; Volk et al., 1997). Therefore we have tested the non-linearity correction with the width parameter $w = 1.5$ as well, but did not find significant differences for the overall age of air distributions, their patterns and variations.

3.4 Global distribution and temporal evolution of age of air

The method described in the previous Section was used to derive monthly zonal means of mean age of stratospheric air (AoA) from the MIPAS SF₆ observations. SF₆ individual profiles have been averaged per month over 10° latitude bins on the altitudes of the retrieval grid to derive monthly zonal means. Data outside the altitude range actually seen by MIPAS (e.g. due to cloud contamination) or of low information content have been omitted. The 10° daily or monthly zonal means of mean age of air have a typical standard deviation of 0.6 to 1.2 yr. The standard errors of the mean (SEM) of daily 10° zonal means are in the order of 0.1 to 0.2 yr, while the SEM of monthly zonal means are 0.02 to 0.03 yr. These errors cover random measurement uncertainty and natural variability of the averaged ensemble only. Systematic errors might be present as well which cannot be reduced by averaging; Stiller et al. (2008) have assessed them to be in the order of 0 to -0.5 yr in the lower stratosphere and up to +1 yr above 25 km, thus varying with latitude and altitude, but not with time. Since for the further work we are interested in the temporal evolution of mean age of air at fixed altitude/latitude bins, these systematic errors, although large compared to the SEM, will not affect our analysis.

Observed temporal evolution of global age of air

G. P. Stiller et al.

Title Page

Abstract

Introduction

Conclusions

References

Tables

Figures

◀

▶

◀

▶

Back

Close

Full Screen / Esc

Printer-friendly Version

Interactive Discussion



Observed temporal evolution of global age of air

G. P. Stiller et al.

Title Page

Abstract

Introduction

Conclusions

References

Tables

Figures

◀

▶

◀

▶

Back

Close

Full Screen / Esc

Printer-friendly Version

Interactive Discussion



While for the first period of MIPAS observations (2002 to 2004) the temporal coverage is still fairly sparse (about 3 to 10 days per month), the second period was almost completely analysed and daily zonal mean age of air data are available for all measurement days in the NOM and UTLS mode of MIPAS. Figure 3 provides a latitude-time cross-section of observed age of air at an altitude of 25 km from pole to pole for September 2002 to January 2010. The age of air distribution reveals the main expected features: lower age in the tropics and high age in the polar regions, pronounced seasonal cycles from the subtropics to the polar latitudes, partly overlaid by a QBO signal which is more pronounced in the Southern Hemisphere than in the Northern Hemisphere. The temporal evolution of mean age of air and its dependence on latitude and altitude will be explored in the next Sections.

4 Analysis of the temporal variation of age of air

4.1 Method

Time series of monthly mean AoA at specific altitudes and for 10° latitude bins have been analysed by fitting the following regression function to the data:

$$\text{age}(t) = a + bt + c_1 \text{qbo}_1(t) + d_1 \text{qbo}_2(t) + \sum_{n=2}^9 \left(c_n \sin \frac{2\pi t}{l_n} + d_n \cos \frac{2\pi t}{l_n} \right) \quad (4)$$

where t is time, qbo_1 and qbo_2 are quasi-biennial oscillation (QBO) indices, and the terms under the sum are 8 sinusoidal functions of the period length l_n . The first two sinusoidal functions have the periods 12 and 6 months, respectively, and represent the seasonal and the semi-annual cycle. The following 6 terms have period lengths of 3, 4, 8, 9, 18 and 24 months and are used to describe deviations

of the temporal variation from a pure sine or cosine relationship, e.g. to model a more saw-tooth like seasonal variation, and to include corrections to the QBO variations. Sine and cosine of the same period length are used together to represent any phase shift of the variation. The terms qbo_1 and qbo_2 are the normalized Singapore winds at 30 and 50 hPa as provided by the Free University of Berlin via <http://www.geo.fu-berlin.de/met/ag/strat/produkte/qbo/index.html>. qbo_1 and qbo_2 are approximately orthogonal such that their combination can emulate any QBO phase shift (Kyrölä et al., 2010). Coefficients a , b , c_1 , ..., c_9 , d_1 , ..., d_9 are fitted to the data using the method of von Clarmann et al. (2010), where the full error covariance matrix of mean age data \mathbf{S}_m is considered, with the squared SEM of the monthly zonal means as the diagonal terms. For the moment, covariances are only important to consider any residual bias between pre-2004 and post-2004 age measurements because of the change of the MIPAS measurements. These residual biases may occur beyond the simple correction of SF_6 volume mixing ratios derived from the tropical tropospheric time series in the first step (see Sect. 3.1) and may be dependent on altitude and latitude. For each time series at a certain altitude and latitude band, the residual bias can simply be treated as a fully correlated error component of one of both data subsets. Tests have shown that, contrary to a simple correction of the residual bias, this method is very robust with respect to the estimate of the residual bias used to create the covariance matrix. Consideration of the residual bias in the covariance matrix is equivalent to infer the residual bias from the data themselves using an optimal estimation scheme where the a priori variance of the residual bias equals the residual bias component in our covariance matrix (cf. von Clarmann et al., 2001). Our method, however, supports consideration of multiple error correlations of different source without formally increasing the number of fit variables. In a later step the consideration of covariances will also be used to handle auto-correlations of fit residuals (see Sect. 7). In any case, the error of the linear trend σ_{Trend} is simply estimated by means of generalized Gaussian error

Observed temporal evolution of global age of air

G. P. Stiller et al.

Title Page

Abstract

Introduction

Conclusions

References

Tables

Figures

◀

▶

◀

▶

Back

Close

Full Screen / Esc

Printer-friendly Version

Interactive Discussion



propagation:

$$\sigma_{\text{Trend}}^2 = \left(\frac{\partial b}{\partial \text{age}_1}, \dots, \frac{\partial b}{\partial \text{age}_n} \right) \mathbf{S}_m \begin{pmatrix} \frac{\partial b}{\partial \text{age}_1} \\ \vdots \\ \frac{\partial b}{\partial \text{age}_n} \end{pmatrix} \quad (5)$$

For more details on the method we refer to von Clarmann et al. (2010). Figure 4 shows examples of AoA time series for 4 different latitude bands and 3 altitudes. The simple model according to Eq. (4) is able to represent the observations very well in most cases. For some latitude/altitude bins, however, large residuals point towards insufficient performance of the regression model. These altitude/latitude bins (with residuals more than a factor of 10 larger than average residuals) have been omitted from the further analysis.

The fits are in general better for the data from the second mission period of MIPAS after 2005. The daily mean data of 2002 to 2004 show larger scatter, and the monthly mean data have larger SEMs and follow less clearly the model curve. Due to larger SEM of the monthly zonal means, they are considered within the regression analysis with less weight than the 2005 to 2010 data set. We recall that the 2002 to 2004 data are sparser than the data after 2005, and were to be corrected for a calibration artefact. For these reasons we consider the 2002 to 2004 data set of inferior quality than the 2005 to 2010 data set. In the future, re-processing of the data from level-1b data with corrected calibration will ultimately solve this problem.

For all altitude/latitude bins, a more or less pronounced seasonal cycle is the dominant feature of the time series. Highest amplitudes of several years are reached in the polar regions, while in the inner tropics, the amplitudes are low. The amplitude of the seasonal cycle reaches a minimum around 20 km which seems to be a “quiet zone”, with increasing amplitudes towards higher and lower altitudes. The semi-annual cycle is most pronounced at higher altitudes, above 30 km. In particular in the Southern Hemisphere, the QBO terms play a larger role, and QBO variations can clearly be identified there. The sine and cosine contributions with other period lengths have

Observed temporal evolution of global age of air

G. P. Stiller et al.

Title Page

Abstract

Introduction

Conclusions

References

Tables

Figures

◀

▶

◀

▶

Back

Close

Full Screen / Esc

Printer-friendly Version

Interactive Discussion



generally low amplitudes and do contribute to the fit mainly by correcting the shape of the dominating oscillations.

Most interesting, however, is the linear increase/decrease which is present in all altitude/latitude bins and varies considerably. In the examples shown here, the linear increase is positive for the Northern mid-latitudes at all altitudes, and the inner tropics and Southern subtropics in the middle stratosphere (25 km), while it is negative for the Northern polar region, and the lower and upper stratosphere in the inner tropics and Southern subtropics. The full global picture will be discussed in the Sect. 6. Before, the potential impact of subsidence of SF₆-depleted mesospheric air in winter polar vortices on the linear increase/decrease for all latitudes will be assessed.

4.2 Impact of SF₆-depleted, downward-transported mesospheric air masses on the age of air distribution

Oldest stratospheric air outside polar vortices is about eight to nine years old. Apparently older air is only observed when mesospheric air subsides into the polar vortex. This is because of a SF₆-sink in the mesosphere (Hall and Waugh, 1998; Reddmann et al., 2001; Stiller et al., 2008), since the low SF₆ abundances are mistaken as indication of very high age. However, in-mixing of subsided SF₆-depleted mesospheric air into the air masses of lower latitudes after the break-down of the polar vortices has the potential to “over-age” also lower latitude air if age is determined from SF₆. The term “apparent age” has been chosen (Waugh and Hall, 2002) to describe age of air which seems to be older than in reality due to in-mixed SF₆-depleted mesospheric air. These intrusions of mesospheric air imply an uncertainty when the Brewer-Dobson circulation is diagnosed by means of the mean apparent age derived from the measured SF₆ amount.

Besides the direct effect on measured apparent versus real age, the mesospheric sink may also have an impact on AoA trends. The mesospheric sink of SF₆ is due to electron-capture and subsequent split of the molecule. As every first-order chemical loss process, it is proportional to the abundance of the reactant SF₆ (and also

Observed temporal evolution of global age of air

G. P. Stiller et al.

Title Page

Abstract

Introduction

Conclusions

References

Tables

Figures

◀

▶

◀

▶

Back

Close

Full Screen / Esc

Printer-friendly Version

Interactive Discussion



to that of the available electrons). Since SF₆ has been increasing strongly over the last decades, it should be expected that SF₆ loss in the mesosphere also has been increased over the last years in absolute terms. This would result in an increasing difference between apparent and real age of air, and it could produce an artificial positive trend in stratospheric age of air, if in-mixing of depleted mesospheric air into hemispheric stratospheric air happens to a noticeable amount. In the following this source of uncertainty is assessed in more detail.

In each polar winter mesospheric air intrudes into the stratospheric polar vortex. During final warming events Southern polar vortices are vertically divided at typically 35 km altitude in an upper and a lower part by mid-latitude air penetrating into polar regions (cf. Fig. 5 and movie in the Supplement). The upper part of the vortex remnant ascends back into the mesosphere while its mixing barriers – discernable as regions of still strong AoA gradients – remain intact. The lower vortex remnant is mixed with mid-latitude air, thus contains air irreversibly subsided from the mesosphere into the stratosphere, affecting the mean age in a sense that through diluted polar ex-mesospheric air the apparent age becomes higher than the true one. Similar behaviour is observed for Northern polar vortices, except that the subsidence of mesospheric air is less pronounced and that the vertical splitting of the vortex is typically not visible in latitudinal means (which certainly does not exclude that it may be present in longitudinally resolved representation). The entire vortex air seems to be mixed into the mid-latitudes. The effect of too large apparent air is also to be considered here.

In the following we quantify the over-aging of non-tropical (polar and mid-latitude) air by mesospheric contamination from estimates of the mean excess age of polar vortex air and the amount of ex-mesospheric air mixed with hemispheric non-tropical air after the final warming for several Northern and Southern winters (Table 1). The volume of the polar vortex was estimated from the positions of the highest vertical and horizontal gradients in the zonal mean age of air distribution. Similarly, the position of the subtropical mixing barrier was estimated from the position of high horizontal gradients in AoA to determine the volume of non-tropical stratospheric air. Excess age

Observed temporal evolution of global age of air

G. P. Stiller et al.

[Title Page](#)[Abstract](#)[Introduction](#)[Conclusions](#)[References](#)[Tables](#)[Figures](#)[Back](#)[Close](#)[Full Screen / Esc](#)[Printer-friendly Version](#)[Interactive Discussion](#)

ranges from 0.03 yr for northern hemispheric winter 2002/2003 to 0.21 yr for southern hemispheric winter 2009. No clear trend in excess age could be determined. Obviously, the amount of air subsided from the mesosphere varies strongly, since it depends on the volume of the polar vortices, and the altitude down to which mesospheric air subsides, which both seem to be very variable from year to year.

A second aspect is that over-aging obviously accumulates over the years since after each winter, SF₆-depleted air is mixed again into the stratospheric air at lower latitudes. The effect of accumulative over-aging over the years could not be quantified in detail because we have no sufficient knowledge on the detailed nature of net fluxes from the stratosphere into the troposphere. The mean age of stratospheric air of 5 yr, however, suggests that 5 contamination events per hemisphere have to be considered. With the numbers of Table 1, we assessed the over-aging of Southern Hemisphere non-tropical air after 5 contaminations at 0.8 yr, and the Northern Hemisphere non-tropical air at 0.4 yr. Extending the in-mixing to the equator (i.e. doubling of air volume) gives an average over-aging per contamination event of 0.08 yr for the Southern Hemisphere and 0.04 yr for the Northern Hemisphere.

Thus, we have corrected monthly mean southern hemispheric (northern hemispheric) AoA data by an amount of -0.08 (-0.04) yr per year of age to account for the accumulative over-aging the air parcel has experienced in its stratospheric “lifetime”. We performed the same analysis of the corrected AoA data set as described in Sect. 4.1 and obtained similar results. As an example, Fig. 6 compares the time series of AoA for 30 to 40° N, 24 km which has been corrected for average over-aging (top) with the original one (bottom). The absolute AoA values have been reduced by about 0.2 yr. The linear increase, however, remained unchanged within its uncertainties (for this example, (0.59 ± 0.08) yr decade⁻¹ for the corrected time series versus (0.61 ± 0.08) yr decade⁻¹ for the uncorrected time series). We conclude therefore, that in-mixing of mesospheric SF₆-depleted air plays a minor role for the assessment of AoA trends, at least within the framework of our approach.

Observed temporal evolution of global age of air

G. P. Stiller et al.

Title Page

Abstract

Introduction

Conclusions

References

Tables

Figures

◀

▶

◀

▶

Back

Close

Full Screen / Esc

Printer-friendly Version

Interactive Discussion



5 Amplitudes and phases of the seasonal variation

Figure 7 presents the amplitudes and phases of the seasonal variation of age of air, as derived by the regression method outline in Sect. 4. We used the uncorrected original data here in order to avoid to introduce any bias or artefacts in the data since our estimate for over-aging correction is still rather crude. The phases of the seasonal variation has been determined from the amplitudes of sine and cosine terms with period length 1 yr. The bottom panel of Fig. 7 indicates how phases have to be read: positive phases shift the maximum of AoA from boreal spring to boreal winter (+0.25 yr) and boreal fall (+0.5 yr), while negative phases shift it to boreal summer (-0.25 yr) and boreal fall (-0.5 yr).

The amplitudes of the seasonal variation of AoA are strongest in the polar regions. This is to be expected due to the intrusion of old and possibly SF₆-depleted mesospheric air into the stratosphere during winter. The phase shifts indicate that oldest air is observed in hemispheric spring in the Southern Hemisphere, and hemispheric late winter to spring in the Northern Hemisphere. At altitudes below approx. 25 km, air is oldest in northern hemispheric spring and early summer for the Northern Hemisphere, and youngest in hemispheric winter, so that a phase shift of almost half a year appears at Northern polar latitudes between 20 and 30 km. This indicates that air below approx. 25 km in the vortex is quite well isolated from subsiding mesospheric air, i.e. subsidence usually does not reach such far down.

While seasonal amplitudes of AoA are large over wide parts of the Southern mid-latitudes, there is a region in the Northern Hemisphere with very small and almost zero seasonal variation. This indicates that the southern hemispheric mid-latitudes above approx. 25 km are well coupled to the polar vortex, and significant in-mixing of vortex air with a strong seasonal cycle takes place. Close to the polar vortex, the southern hemispheric mid-latitudes are more or less in phase with the vortex air (phase shift of +0.5 yr and -0.5 yr results in the same), while at lower latitudes (at 50° S–30° S, 20–30 km), oldest air is observed in hemispheric summer.

Observed temporal evolution of global age of air

G. P. Stiller et al.

Title Page

Abstract

Introduction

Conclusions

References

Tables

Figures

◀

▶

◀

▶

Back

Close

Full Screen / Esc

Printer-friendly Version

Interactive Discussion



In the Northern mid-latitude middle stratosphere, the seasonality of age of air is coupled to the tropics, and youngest air (oldest air) occurs in winter (summer), i.e. a phase shift of almost half a year with respect to the polar region is present, similar to the Southern Hemisphere.

Both the Northern and the Southern tropics show a very small seasonality with amplitudes close to zero, and the phase indicates youngest air in boreal winter. This is expected for the northern hemispheric Brewer-Dobson circulation which exhibits strongest upwelling in boreal winter, however it is interesting to see that the Southern tropics are in phase with the Northern tropics. The only exception in the Southern tropics is the region between 0 and 20° S below 21 km where youngest air is observed in the austral, not boreal winter.

An interesting region is the band of high seasonal amplitudes in the Northern Hemisphere which starts around 20–30° N, 17 km and stretches to 50–60° N, 40 km. This region is roughly in phase with the tropics and the remaining Northern mid-latitudes, and is surrounded of regions with low seasonal amplitudes, so that in-mixing of air with high seasonality, as it is the case at the vortex boundary, cannot explain the high amplitudes. We speculate that a seasonality in the position or the strength of the subtropical mixing barrier produces the strong seasonal variation in this region, so that the air sampled in this region is of tropical origin in winter when it is youngest, and of mid-latitudinal origin in summer when it is oldest (compare also Fig. 3).

The mid-latitude lowermost stratospheres in both hemispheres are other interesting regions. In the Northern Hemisphere, the seasonal amplitudes are high, and the phase is shifted by half a year with respect to its surroundings, i.e. youngest air is found in summer. We interpret this as indication that the shallow branch of the Brewer-Dobson circulation which transports air within the so-called “tropically controlled transition region” (Rosenlof et al., 1997; Birner and Bönisch, 2011; Bönisch et al., 2011) dominates here. The subtropical jet is weakest and most permeable in summer, allowing intrusion of young tropical air into the mid-latitudinal lowermost stratosphere in summer. The seasonality in the mid-latitudinal lowermost stratosphere thus is caused by the variation

Observed temporal evolution of global age of air

G. P. Stiller et al.

Title Page

Abstract

Introduction

Conclusions

References

Tables

Figures

◀

▶

◀

▶

Back

Close

Full Screen / Esc

Printer-friendly Version

Interactive Discussion



of the permeability of the subtropical jet with season.

Although we see a similar phase shift of half a year towards southern hemispheric summer for the mid-latitudinal lowermost stratosphere in the Southern Hemisphere, the seasonal amplitudes remain small there. This can either mean that the exchange through the Southern subtropical jet is less effective, or that the contrast of age of air between the Southern tropics and the Southern mid-latitudes is smaller than in the Northern Hemisphere.

6 Altitude- and latitude dependence of the linear increase/decrease

We understand the linear increase/decrease (in the following: linear increase) derived from our regression analysis as the joint effect of all atmospheric variability which can be expressed by a linear regression function and which cannot be characterised by the QBO term or the periodics under consideration. It is strictly valid for the observation period of 2002 to 2010 only, thus we hesitate to call it “trend”. As already obvious from Fig. 4, the linear increase of AoA is by far not homogeneous over altitudes and latitudes, but reveals a significant variation. The global view is presented in Fig. 8, top panel. Red areas indicate increasing AoA, while blue regions indicate decreasing AoA. A large contiguous region of increasing AoA is seen in the non-polar Northern stratosphere over all altitudes and the mid-stratosphere (22 to 32 km) tropics and Southern mid-latitudes. Further, the Southern polar region at high altitudes also reveals an increasing AoA. In contrast, the lowermost and upper tropical stratosphere, the Northern polar regions, and some parts of Southern higher latitudes show decreasing age of air for the 2002 to 2010 period. The uncertainties are small (see Fig. 8, middle panel) and the results are significant on the $2\text{-}\sigma$ or better level for most of the altitude/latitude bins (see Fig. 8, bottom panel). The vertical profiles of AoA linear variation for every second latitude bin are shown in Fig. 9, together with their $2\text{-}\sigma$ uncertainties.

Engel et al. (2009) derived a trend of AoA for 30 to 50° N of $+0.24 \pm 0.22$ yr per decade ($1\text{-}\sigma$ uncertainty level) for the 24 to 35 km altitude range. For the Northern

Observed temporal evolution of global age of air

G. P. Stiller et al.

Title Page

Abstract

Introduction

Conclusions

References

Tables

Figures



Back

Close

Full Screen / Esc

Printer-friendly Version

Interactive Discussion



mid-latitudes in the 24 to 35 km altitude region, the linear increase derived from MIPAS data is significantly larger on the $1\text{-}\sigma$ level (see Fig. 9), and just consistent on the $2\text{-}\sigma$ level, to that derived by Engel et al. (2009) (compare also Fig. 6). For Northern mid-latitudes, the AoA increase derived from MIPAS is significantly distinct from zero for all altitudes. The observed increase of Northern mid-latitudinal AoA as presented first by Engel et al. (2009) is thus confirmed by our observations, the steepness of the increase, however, is even larger in our data set than in the 30-yr data record of Engel et al. (2009). Regarding this discrepancy, one has to keep in mind, however, that the observed time intervals have only little overlap: the Engel et al. (2009) data set covers the years 1975 to 2005, while MIPAS covers the years 2002 to 2010. Although Engel et al. (2009) did not discuss any indication of the impact of solar cycle variability, we must also keep in mind that the MIPAS time series covers the declining phase of solar cycle 23 and the deep minimum after 2008 only. Due to this coincidence, any solar signal in the global circulation which may occur, according to e.g. Kodera and Kuroda (2002) or Labitzke (1987), could not be separated from the longer-term variation and thus may be hidden in the linear increase.

The MIPAS-derived AoA increase is highly inconsistent to model results. The results of model calculations published so far indicate consistently a decrease in age of air over past decades and predict further decrease for future decades (Waugh, 2009; Austin and Li, 2006; Garcia et al., 2011; SPARC CCMVal, 2010). E.g. Waugh (2009) presented a compilation of model results for Northern mid-latitudes covering the years 1960 to 2005; they showed consistently an acceleration of the Brewer-Dobson circulation expressed as a decrease of age of air from -0.05 to -0.20 yr decade⁻¹, which is in sharp contrast to the observed increase presented in this study.

Recent model results (Garcia et al., 2011) present the variation of age of air for the mid-latitude stratosphere (40.7° N, 20 hPa) and the tropical middle stratosphere (0.9° N, 10.7 hPa) and obtain for both locations statistically significant over-all decreases of AoA. The time series, however, show considerable variation in the steepness of the decrease, and even shorter-term periods (of approx. 5 yr) for which AoA increases.

Observed temporal evolution of global age of air

G. P. Stiller et al.

Title Page

Abstract

Introduction

Conclusions

References

Tables

Figures

◀

▶

◀

▶

Back

Close

Full Screen / Esc

Printer-friendly Version

Interactive Discussion



For the period 2000 to 2006, however, the trend is negative in all presentations of model results in this paper.

Randel et al. (2006) concluded from observations of water vapor and temperature in the tropical lower stratosphere after 2001, that the upwelling across the tropical tropopause should have increased, and linked this observation to an intensification of the Brewer-Dobson circulation. Randel and Thompson (2011) confirmed these findings on basis of tropical ozone observations, and extended the relevant period to 1984 to 2009. These observations are consistent to the findings from our data analysis, since indeed we derive decreasing age of air in the lowermost stratosphere below 22 km from 30° S to 20° N. Decreasing AoA was also found in the upper part of the tropical pipe above 32 km, but not in the intermediate region of 22 to 32 km.

Several attempts have been made to resolve the contradiction between the Engel et al. (2009) observations and the model results. Ray et al. (2010) introduced the so-called “Leaky tropical pipe model” including a term that allows mixing of air from the mid-latitudes into the tropics to be consistent with observations of the tropical stratosphere. They found that the best quantitative agreement with observed mean age and ozone trends was achieved assuming a small strengthening of the mean circulation in the lower stratosphere, a moderate weakening of the mean circulation in the middle and upper stratosphere, and a moderate increase in the horizontal mixing into the tropics. They also found that the mean age of air trends are strongly sensitive to trends in the horizontal mixing into the tropics.

Applied to our observations, strengthening of the mean circulation together with weakening of mixing barriers would be a plausible hypothesis to explain the pattern of increasing and decreasing AoA over altitudes/latitudes as shown in Fig. 8, top panel. Weakening of the mixing barrier along the Northern polar vortex would cause polar air becoming younger, and mid-latitudinal air becoming older. Weakening of the subtropic mixing barrier in the middle stratosphere would cause middle stratospheric tropical air becoming older, while increased upwelling due to intensified Brewer-Dobson circulation would result in younger air in the lowermost and uppermost tropical stratosphere,

Observed temporal evolution of global age of air

G. P. Stiller et al.

Title Page

Abstract

Introduction

Conclusions

References

Tables

Figures



Back

Close

Full Screen / Esc

Printer-friendly Version

Interactive Discussion



regions which were not affected by changes in the strength of the subtropical mixing barrier. Changes in the strength of the mixing barriers then would obviously be less pronounced in the Southern Hemisphere, since areas with decreasing age of air – consistent to an intensification of the Brewer-Dobson circulation – are found in the Southern mid-latitudes. The Southern polar vortex air is becoming older as expected from in-mixing of increasingly stronger SF₆-depleted air as outlined in Sect. 4.2. Within this scenario, longer-term weakening of the mixing barriers formed by the subtropical jets seems not to be confirmed, since mid-latitude air in the lowermost stratosphere is becoming older, i.e. a direct coupling to the air with decreasing age in the lowermost tropical stratosphere is not very probable. This result is in contradiction to findings of Birner and Bönisch (2011) and Bönisch et al. (2011) who deduced an intensification of the shallow branch of the Brewer-Dobson circulation from observations and transit-time calculations.

7 Impact of empirical errors and autocorrelation

As already said, linear increases/decreases analysed so far are understood as the joint effect of all atmospheric variability which can be expressed by a linear regression function and which cannot be characterised by the QBO term or the periodics under consideration. Uncertainties under consideration were only the standard errors of the monthly zonal means of AoA data and the bias between the MIPAS high- versus low spectral resolution measurement periods. No error of the regression model was considered. Fit residuals larger than the error bars of the data points, however, suggest that the regression model does not perfectly describe atmospheric variability. In order to truly infer the linear increase (in the climatological sense) and its uncertainty, we now additionally consider an error component characterizing the uncertainty caused by the regression model error not fully representing the observed variability. This error component was chosen such that the observed variance of the residuals was consistent with the combined standard errors of the monthly means and the regression model error. Covariances between next and some further neighbours of datapoints in

Observed temporal evolution of global age of air

G. P. Stiller et al.

Title Page

Abstract

Introduction

Conclusions

References

Tables

Figures



Back

Close

Full Screen / Esc

Printer-friendly Version

Interactive Discussion



the time series were considered as long as the correlations were larger than 0.01 (in absolute terms) in order to account for possible auto-correlations between the monthly means; however, autocorrelations among data points of the time series (i.e. the monthly means) were found to be small in general. Auto-correlations among single measurements which were averaged to build the daily or monthly means, and which would increase their SEMs, were small as well and could be neglected. Numerical experiments where model fields were sampled according to the MIPAS sampling patterns gave no evidence that standard errors of monthly zonal means calculated without consideration of auto-correlation would be systematically too optimistic (M. Toohey, personal communication, 2011). On the contrary, in the case of the sampling patterns of MIPAS full spectral resolution measurements, the average correlation coefficients of autocorrelation seem even to be negative, rendering the simplified estimates of the SEM too pessimistic.

Contrary to the observation-error based linear increase/decrease as presented in the previous Section, which represents the linear approximation of the superposition of multiple atmospheric variations leading to any kind of long-term change, we call the change of age with time derived under consideration of all non-linear and unaccounted atmospheric variation as regression model error “model-error corrected linear increase” (see Fig. 10, upper panel). The individual results for each altitude/latitude bin change slightly compared to the linear increase shown in Fig. 8, the overall patterns, however, remain similar, at least below 30 km. As expected, evidence of a significant model-error corrected linear increase is detected not as frequent as evidence of a significant observation-error based linear increase (Fig. 10, lower panel). Nevertheless, the consistency of the linear increase/decrease patterns in Fig. 8 and Fig. 10, and the fact that regions of increasing versus decreasing age of air are contiguous over latitudes and altitudes in Fig. 10 provide some indication for the reliability of the age of air multi-year linear variation derived under consideration of model errors. The positive linear increases of AoA in the stratosphere between 20 and 30 km and 30° S and 60° N, however, are confirmed on a 2- σ or better confidence level anyhow.

Observed temporal evolution of global age of air

G. P. Stiller et al.

[Title Page](#)[Abstract](#)[Introduction](#)[Conclusions](#)[References](#)[Tables](#)[Figures](#)[◀](#)[▶](#)[◀](#)[▶](#)[Back](#)[Close](#)[Full Screen / Esc](#)[Printer-friendly Version](#)[Interactive Discussion](#)

8 Conclusions

More than 10^6 SF₆ profiles were retrieved from MIPAS limb emission mid-infrared spectral data (ESA version 4.61 up to 4.67) over the observation period of 2002 to January 2010. The retrieval procedure followed in general Stiller et al. (2008), and only few adjustments were made to account for the reduced spectral resolution of MIPAS data after 2005. Mean age of stratospheric air was derived from the SF₆ data by referencing any stratospheric SF₆ observation to the time the same SF₆ amount had been observed in the troposphere, represented by a global mean derived from a global network of NOAA/ESRL insitu and flask observations (Hall et al., 2011). Since the tropospheric SF₆ did not increase strictly linearly over the last years, a non-linearity correction was applied in the age of air derivation which iteratively searched for that age of air which is consistent to the observed SF₆ after convolution with the age spectrum. The applied corrections, however, were in general smaller than 0.2 yr.

Time series of monthly zonal means of age of air on 10° latitude bins and 1–2 km altitude bins were analysed with a regression function including a constant and a linear term, two QBO proxy terms, and 8 sine and cosine terms, the first two of which represent the seasonal and the semi-annual variations. The global distributions of linear increases/decreases, and seasonal amplitudes and phases reveal considerable variation over the globe with areas of increasing as well as decreasing age of air. Seasonal amplitudes of up to 2 yr occur in the global age of air distribution, with highest amplitudes in the polar regions and lowest amplitudes in the tropics. The high seasonality in the polar regions comes from the intrusion of old, but possibly also SF₆-depleted, mesospheric air during polar winter the latter of which causes an “over-aging” of polar air. The impact of “over-aged” (i.e. apparently older than in reality) polar air on both the age of air and its linear increase/decrease at lower latitudes was assessed and found to be small: the age of air was shifted by about –0.2 yr, while the linear increase/decrease was affected within its uncertainties only. High seasonality in the southern hemispheric mid-litudinal upper stratosphere indicates a considerable

Observed temporal evolution of global age of air

G. P. Stiller et al.

[Title Page](#)[Abstract](#)[Introduction](#)[Conclusions](#)[References](#)[Tables](#)[Figures](#)[⏪](#)[⏩](#)[◀](#)[▶](#)[Back](#)[Close](#)[Full Screen / Esc](#)[Printer-friendly Version](#)[Interactive Discussion](#)

Observed temporal evolution of global age of air

G. P. Stiller et al.

[Title Page](#)[Abstract](#)[Introduction](#)[Conclusions](#)[References](#)[Tables](#)[Figures](#)[◀](#)[▶](#)[◀](#)[▶](#)[Back](#)[Close](#)[Full Screen / Esc](#)[Printer-friendly Version](#)[Interactive Discussion](#)

coupling of these air masses to the polar region, i.e. in-mixing of old polar air after the break-down of the polar vortex occurs regularly. Other regions of high seasonality are a band in the Northern mid-latitudes which might obtain its seasonality from the subtropical mixing barrier shifting its position or varying its strength within a seasonal cycle, and the lowermost stratosphere in the Northern mid-latitudes, which obtains its seasonality from the permeability of the subtropical jet with highest permeability (and youngest air in mid-latitudes) in late summer. The analysis of the phases of the seasonal variation indicates, that most of the Northern mid-latitudes follow the tropics in their phase, i.e. have youngest air in (late) winter, in accordance with the more intensive Brewer-Dobson circulation in the winter hemisphere. Southern mid-latitudes are influenced from the polar regions, thus having their youngest air in Southern winter and oldest air after break-down of the polar vortex. The polar regions have their oldest air in Southern spring and Northern late winter. The linear increases/decreases are similarly inhomogeneous over the latitudes and altitudes: we find increasing age of air for the Southern polar region, most of the Northern mid-latitudes and the lower to middle tropical stratosphere, while age of air is decreasing for the lowermost and upper tropical stratosphere, some areas in the Southern mid-latitudes and the Northern polar region. Decrease of age of air in the tropical lowermost stratosphere is consistent to earlier observational evidence of increased tropical upwelling, derived from observations of tropical lower stratospheric water vapor and ozone and tropopause temperatures. The unchanged or, if any, increasing age of air as derived by Engel et al. (2009) is confirmed as well, with even steeper and statistically significant increases. The overall complicated pattern age of air increase/decrease might, as a hypothesis, be consistent with a general increasing upwelling in the tropics and intensification of the Brewer-Dobson circulation, but simultaneous weakening of the subtropical and polar mixing barriers. A stricter analysis of our data, taking model errors and autocorrelation within the data points into account, provides a similar picture, however with reduced significance of the mean linear increase. Nevertheless, a wide region in the tropical to mid-latitudinal lower to middle stratosphere (20 to 30 km) exhibits a positive mean linear increase of

age of air, with $2\text{-}\sigma$ or better significance.

In any case, the global picture of age of air and its temporal variation demonstrates that there is not one positive or negative linear variation of age of air over the globe. Future comparisons between observations and models should take these inhomogeneities into account.

The data material presented in this paper, i.e. the monthly zonal means of mean age of stratospheric air, is available as netcdf data files from the authors upon request, and a movie showing the temporal evolution of altitude-latitude cross-sections of mean age of air is provided in the Supplement.

Supplementary material related to this article is available online at:
**[http://www.atmos-chem-phys-discuss.net/11/28013/2011/
acpd-11-28013-2011-supplement.zip](http://www.atmos-chem-phys-discuss.net/11/28013/2011/acpd-11-28013-2011-supplement.zip)**

Acknowledgements. We would like to acknowledge provision of MIPAS level-1b data by ESA. The provision of sulfur hexafluoride data from the NOAA/ESRL halocarbons in situ program is gratefully acknowledged. We thank the PIs of the program, Bradley Hall, Geoff Dutton, and James W. Elkins II, for their support with using their data and their helpful comments on the manuscript. The work presented in this paper was funded via the “CAWSES” priority program of the German Research Foundation (DFG) within the project “Tracers and mean age”. This work is also a contribution to the DFG research unit “SHARP – Stratospheric Change and its Role for Climate Prediction”. Development of SF₆ data retrieval was partly funded by the German Federal Ministry of Education and Research (BMBF) via contract no. 50EE0901. GPS would like to thank Greg Bodecker for helpful discussions regarding autocorrelation of data.

**Observed temporal
evolution of global
age of air**

G. P. Stiller et al.

Title Page

Abstract

Introduction

Conclusions

References

Tables

Figures

◀

▶

◀

▶

Back

Close

Full Screen / Esc

Printer-friendly Version

Interactive Discussion



References

- Andrews, A. E., Boering, K. A., Daube, B. C., Wofsy, S. C., Hints, E. J., Weinstock, E. M., and Bui, T. P.: Empirical age spectra for the lower tropical stratosphere from in situ observations of CO₂: Implications for stratospheric transport, *J. Geophys. Res.*, 104, 26581–26595, 1999. 28022
- Austin, J. and Li, F.: On the relationship between the strength of the Brewer-Dobson circulation and the age of stratospheric air, *Geophys. Res. Lett.*, 33, L17807, doi:10.1029/2006GL026867, 2006. 28015, 28016, 28034
- Austin, J., Wilson, J., Li, F., and Vömel, H.: Evolution of water vapor and age of air in coupled chemistry climate model simulations of the stratosphere, *J. Atmos. Sci.*, 64, 905–921, 2007. 28015
- Baldwin, M. P., Dameris, M., and Shepherd, T. G.: How will the Stratosphere affect climate change?, *Science*, 316, 1576–1577, doi:10.1126/science.1144303, 2007. 28015
- Birner, T. and Bönisch, H.: Residual circulation trajectories and transit times into the extratropical lowermost stratosphere, *Atmos. Chem. Phys.*, 11, 817–827, doi:10.5194/acp-11-817-2011, 2011. 28032, 28036
- Bönisch, H., Engel, A., Birner, Th., Hoor, P., Tarasick, D. W., and Ray, E. A.: On the structural changes in the Brewer-Dobson circulation after 2000, *Atmos. Chem. Phys.*, 11, 3937–3948, doi:10.5194/acp-11-3937-2011, 2011. 28032, 28036
- Butchart, N. and Scaife, A. A.: Removal of chlorofluorocarbons by increased mass exchange between the stratosphere and troposphere in a changing climate, *Nature*, 410, 799–802, doi:10.1038/35071047, 2001. 28015
- Butchart, N., Scaife, A. A., Bourqui, M., de Grandpre, J., Hare, S. H. E., Kettleborough, J., Langematz, U., Manzini, E., Sassi, F., Shibata, K., Shindell, D., and Sigmond, M.: Simulations of anthropogenic change in the strength of the Brewer-Dobson circulation, *Clim. Dynam.*, 27, 727–741, doi:10.1007/s00382-006-0162-4, 2006. 28015
- Dhomse, S., Weber, M., and Burrows, J.: The relationship between tropospheric wave forcing and tropical lower stratospheric water vapor, *Atmos. Chem. Phys.*, 8, 471–480, doi:10.5194/acp-8-471-2008, 2008. 28015
- Douglass, A. R., Stolarski, R. S., Schoeberl, M. R., Jackman, C. H., Gupta, M. L., Newman, P. A., Nielsen, J. E., and Fleming, E. L.: Relationship of loss, mean age of air and the distribution of CFCs to stratospheric circulation and implications for atmospheric lifetimes, *J.*

Observed temporal evolution of global age of air

G. P. Stiller et al.

Title Page

Abstract

Introduction

Conclusions

References

Tables

Figures

◀

▶

◀

▶

Back

Close

Full Screen / Esc

Printer-friendly Version

Interactive Discussion



- Geophys. Res., 113, D14309, doi:10.1029/2007JD009575, 2008. 28015
- Elkins, J. W. and Dutton, G. S.: Nitrous oxide and sulfur hexafluoride [in “State of the Climate in 2008”], Bull. Amer. Meteor. Soc., 90, S38–S39, 2009. 28020
- Engel, A., Strunk, M., Müller, M., Haase, H.-P., Poss, C., Levin, I., and Schmidt, U.:
5 Temporal development of total chlorine in the high-latitude stratosphere based on reference distributions of mean age derived from CO₂ and SF₆, J. Geophys. Res., 107, D12, doi:10.1029/2001JD000584, 2002. 28016
- Engel, A., Möbius, T., Haase, H.-P., Bönisch, H., Wetter, T., Schmidt, U., Levin, I., Reddman, T., Oelhaf, H., Wetzell, G., Grunow, K., Huret, N., and Pirre, M.: Observation of mesospheric
10 air inside the arctic stratospheric polar vortex in early 2003, Atmos. Chem. Phys., 6, 267–282, doi:10.5194/acp-6-267-2006, 2006. 28016, 28019
- Engel, A., Möbius, T., Bönisch, H., Schmidt, U., Heinz, R., Levin, I., Atlas, E., Aoki, S., Nakazawa, T., Sugawara, S., Moore, F., Hurst, D., Elkins, J., Schauffler, S., Andrews, A., and Boering, K.: Age of stratospheric air unchanged within uncertainties over the past 30
15 years, Nat. Geosci., 2, 28–31, doi:10.1038/ngeo388, 2009. 28014, 28017, 28033, 28034, 28035, 28039, 28053, 28055, 28058
- Fischer, H., Birk, M., Blom, C., Carli, B., Carlotti, M., von Clarmann, T., Delbouille, L., Dudhia, A., Ehhalt, D., Endemann, M., Flaud, J. M., Gessner, R., Kleinert, A., Koopman, R., Langen, J., López-Puertas, M., Mosner, P., Nett, H., Oelhaf, H., Perron, G., Remedios, J., Ridolfi, M., Stiller, G., and Zander, R.: MIPAS: an instrument for atmospheric and climate research,
20 Atmos. Chem. Phys., 8, 2151–2188, doi:10.5194/acp-8-2151-2008, 2008. 28018
- Garcia, R. R. and Randel, W. J.: Acceleration of the Brewer-Dobson Circulation due to Increases in Greenhouse Gases, J. Atmos. Sci., 65, 2731–2739, doi:10.1175/2008JAS2712.1, 2008. 28015
- 25 Garcia, R. R., Randel, W. J., and Kinnison, D. E.: On the determination of age of air trends from atmospheric trace species, J. Atmos. Sci., 68, 139–154, 2011. 28017, 28034
- Hall, B. D., Dutton, G. S., Mondeel, D. J., Nance, J. D., Rigby, M., Butler, J. H., Moore, F. L., Hurst, D. F., and Elkins, J. W.: Improving measurements of SF₆ for the study of atmospheric transport and emissions, Atmos. Meas. Tech. Discuss., 4, 4131–4163, doi:10.5194/amtd-4-4131-2011, 2011. 28020, 28021, 28022, 28038
- 30 Hall, T. M. and Plumb, R. A.: Age as a diagnostic of stratospheric transport, J. Geophys. Res., 99, 1059–1070, 1994. 28024
- Hall, T. M. and Waugh, D. W.: Influence of nonlocal chemistry on tracer distribu-

Observed temporal evolution of global age of airG. P. Stiller et al.

[Title Page](#)[Abstract](#)[Introduction](#)[Conclusions](#)[References](#)[Tables](#)[Figures](#)[◀](#)[▶](#)[◀](#)[▶](#)[Back](#)[Close](#)[Full Screen / Esc](#)[Printer-friendly Version](#)[Interactive Discussion](#)

tions: Inferring the mean age of air from SF₆, *J. Geophys. Res.*, 103, 13327–13336, doi:10.1029/98JD00170, 1998. 28028

IPCC: Contribution of Working Group I to the Fourth Assessment Report of the Intergovernmental Panel on Climate Change, in: *Climate Change 2007: The Physical Science Basis*, edited by: Solomon, S., Qin, D., Manning, M., Chen, Z., Marquis, M., Averyt, K. B., Tignor, M., and Miller, H. L., Cambridge University Press, Cambridge, UK and New York, NY, USA, 996 pp., 2007. 28015

Kodera, K. and Kuroda, Y.: Dynamical response to the solar cycle, *J. Geophys. Res.*, 107, 4749, doi:10.1029/2002JD002224, 2002. 28034

Kyrölä, E., Tamminen, J., Sofieva, V., Bertaux, J. L., Hauchecorne, A., Dalaudier, F., Fussen, D., Vanhellemont, F., Fanton d'Andon, O., Barrot, G., Guirlet, M., Fehr, T., and Saavedra de Miguel, L.: GOMOS O₃, NO₂, and NO₃ observations in 2002–2008, *Atmos. Chem. Phys.*, 10, 7723–7738, doi:10.5194/acp-10-7723-2010, 2010. 28026

Labitzke, K.: Sunspots, the QBO, and the stratospheric temperature in the north polar region, *Geophys. Res. Lett.*, 14, 535–537, 1987. 28034

Levin, I., Naegler, T., Heinz, R., Osusko, D., Cuevas, E., Engel, A., Illmerger, J., Langenfelds, R. L., Neisinger, B., Rohden, C. v., Steele, L. P., Weller, R., Worthy, D. E., and Zimov, S. A.: The global SF₆ source inferred from long-term high precision atmospheric measurements and its comparison with emission inventories, *Atmos. Chem. Phys.*, 10, 2655–2662, doi:10.5194/acp-10-2655-2010, 2010. 28020

Li, S. and Waugh, D. W.: Sensitivity of mean age and long-lived tracers to transport parameters in a two-dimensional model, *J. Geophys. Res.*, 104, 30559–30569, doi:10.1029/1999JD900913, 1999. 28015

McLandress, C. and Shepherd, T. G.: Simulated Anthropogenic Changes in the Brewer-Dobson Circulation, Including its Extension to high latitudes, *J. Climate*, 22, 1516–1540, doi:10.1175/2008JCLI2679.1, 2009. 28015

Oman, L., Waugh, D. W., Pawson, S., Stolarski, R. S., and Newman, P. A.: On the influence of anthropogenic forcings on changes in the stratospheric mean age, *J. Geophys. Res.*, 114, D03105, doi:10.1029/2008JD010378, 2009. 28015

Plumb, R. A., Heres, W., Neu, J. L., Mahowald, N., del Corral, J., Toon, G. C., Ray, E., Moore, F., and Andrews, A. E.: Global tracer modeling during SOLVE: High-latitude descent and mixing, *J. Geophys. Res.*, 107, 8309, doi:10.1029/2001JD001023, printed 108(D5), 2003, 2002. 28016

Observed temporal evolution of global age of air

G. P. Stiller et al.

Title Page

Abstract

Introduction

Conclusions

References

Tables

Figures

◀

▶

◀

▶

Back

Close

Full Screen / Esc

Printer-friendly Version

Interactive Discussion



Randel, W. J. and Thompson, A.: Interannual variability and trends in tropical ozone derived from SAGE II satellite data and SHADOZ ozonesondes, *J. Geophys. Res.*, 116, D07303, doi:10.1029/2010JD015195, 2011. 28015, 28035

Randel, W. J., Wu, F., Vömel, H., Nedoluha, G. E., and Forster, P.: Decreases in stratospheric water vapor after 2001: Links to changes in the tropical tropopause and the Brewer–Dobson circulation, *J. Geophys. Res.*, 111, D12312, doi:10.1029/2005JD006744, 2006. 28015, 28035

Ray, E., Moore, F., Rosenlof, K., Davis, S., Boenisch, H., Morgenstern, O., Smale, D., Rozanov, E., Hegglin, M., Pitari, G., Mancini, E., Braesicke, P., Butchart, N., Hardiman, S., Li, F., Shibata, K., and Plummer, D. A.: Evidence for changes in stratospheric transport and mixing over the past three decades based on multiple data sets and tropical leaky pipe analysis, *J. Geophys. Res.*, 115, D21304, doi:10.1029/2010JD014206, 2010. 28035

Ray, E. A., Moore, F. L., Elkins, J. W., Hurst, D. F., Romashkin, P. A., S.Dutton, G., and Fahey, D. W.: Descent and mixing in the 1999–2000 northern polar vortex inferred from in situ tracer measurements, *J. Geophys. Res.*, 107, 8285, doi:10.1029/2001JD000961, 2002. 28016

Reddmann, T., Ruhnke, R., and Kouker, W.: Three–dimensional model simulations of SF₆ with mesospheric chemistry, *J. Geophys. Res.*, 106, 14525–14537, doi:10.1029/2000JD900700, 2001. 28016, 28028

Rigby, M., Mühle, J., Miller, B. R., Prinn, R. G., Krummel, P. B., Steele, L. P., Fraser, P. J., Salameh, P. K., Harth, C. M., Weiss, R. F., Grealley, B. R., O’Doherty, S., Simmonds, P. G., Vollmer, M. K., Reimann, S., Kim, J., Kim, K.-R., Wang, H. J., Olivier, J. G. J., Dlugokencky, E. J., Dutton, G. S., Hall, B. D., and Elkins, J. W.: History of atmospheric SF₆ from 1973 to 2008, *Atmos. Chem. Phys.*, 10, 10305–10320, doi:10.5194/acp-10-10305-2010, 2010. 28020

Rosenlof, K. H. and Reid, G. C.: Trends in the temperature and water vapor content of the tropical lower stratosphere: Sea surface connection, *J. Geophys. Res.*, 113, D06107, doi:10.1029/2007JD009109, 2008. 28015

Rosenlof, K. H., Tuck, A. F., Kelly, K. K., Russell III, J. M., and McCormick, M. P.: Hemispheric asymmetries in water vapor and inferences about transport in the lower stratosphere, *J. Geophys. Res.*, 102, 13213–13234, 1997. 28032

Schoeberl, M. R., Douglass, A. R., Polansky, B., Boone, C., Walker, K. A., and Bernath, P.: Estimation of stratospheric age spectrum from chemical tracers, *J. Geophys. Res.*, 110, D21303, doi:10.1029/2005JD006125, 2005. 28024

Shepherd, T. G.: Dynamics, Stratospheric Ozone, and Climate Change, *Atmos.-Ocean*, 46,

Observed temporal evolution of global age of air

G. P. Stiller et al.

Title Page

Abstract

Introduction

Conclusions

References

Tables

Figures

◀

▶

◀

▶

Back

Close

Full Screen / Esc

Printer-friendly Version

Interactive Discussion



117–138, doi:10.3137/ao.460106, 2008. 28015

Solomon, S., Rosenlof, K. H., Portmann, R. W., Daniel, J. S., Davis, S. M., Sanford, T. J., and Plattner, G.-K.: Contributions of Stratospheric Water Vapor to Decadal Changes in the Rate of Global Warming, *Science*, 327, 1219–1223, doi:10.1126/science.1182488, 2010. 28015

5 SPARC CCMVal: Neu, J. and Strahan, S., Chapter 5. Transport, in: SPARC Report on the Evaluation of Chemistry-Climate Models, edited by: Eyring, V., Shepherd, T. G., and Waugh, D. W., SPARC Report No. 5, WCRP-132, WMO/TD-No. 1526, <http://www.atmosp.physics.utoronto.ca/SPARC>, 2010. 28015, 28034

Steck, T. and von Clarmann, T.: Constrained profile retrieval applied to the observation mode of the Michelson Interferometer for Passive Atmospheric Sounding, *Appl. Opt.*, 40, 3559–3571, 2001. 28018

10 Stiller, G. P., von Clarmann, T., Höpfner, M., Glatthor, N., Grabowski, U., Kellmann, S., Kleinert, A., Linden, A., Milz, M., Reddmann, T., Steck, T., Fischer, H., Funke, B., López-Puertas, M., and Engel, A.: Global distribution of mean age of stratospheric air from MIPAS SF₆ measurements, *Atmos. Chem. Phys.*, 8, 677–695, doi:10.5194/acp-8-677-2008, 2008. 28016, 28018, 28019, 28024, 28028, 28038

15 Strunk, M., Engel, A., Schmidt, U., Volk, C. M., Wetter, T., Levin, I., and Glatzel-Mattheier, H.: CO₂ and SF₆ as stratospheric age tracers: consistency and the effect of mesospheric SF₆-loss, *Geophys. Res. Lett.*, 27, 341–344, doi:10.1029/1999GL011044, 2000. 28016

20 Thompson, D. W. J. and Solomon, S.: Recent stratospheric climate trends as evidenced in radiosonde data: Global structure and tropospheric linkages, *J. Climate*, 18, 4785–4795, doi:10.1175/JCLI3585.1, 2005. 28015

Tikhonov, A.: On the solution of incorrectly stated problems and method of regularization, *Dokl. Akad. Nauk. SSSR*, 151, 501–504, 1963. 28018

25 Volk, C. M., Elkins, J. W., Fahey, D. W., Dutton, G. S., Gilligan, J. M., Loewenstein, M., Podolske, J. R., Chan, K. R., and Gunson, M. R.: Evaluation of source gas lifetimes from stratospheric observations, *J. Geophys. Res.*, 102, 25,543–25,564, doi:10.1029/97JD02215, 1997. 28023, 28024

30 von Clarmann, T., Grabowski, U., and Kiefer, M.: On the role of non-random errors in inverse problems in radiative transfer and other applications, *J. Quant. Spectrosc. Radiat. Transfer*, 71, 39–46, 2001. 28026

von Clarmann, T., Stiller, G., Grabowski, U., Eckert, E., and Orphal, J.: Technical Note: Trend estimation from irregularly sampled, correlated data, *Atmos. Chem. Phys.*, 10, 6737–6747,

Observed temporal evolution of global age of air

G. P. Stiller et al.

Title Page

Abstract

Introduction

Conclusions

References

Tables

Figures

◀

▶

◀

▶

Back

Close

Full Screen / Esc

Printer-friendly Version

Interactive Discussion



doi:10.5194/acp-10-6737-2010, 2010. 28026, 28027

Waugh, D.: The age of stratospheric air, *Nat. Geosci.*, 2, 14–16, 2009. 28015, 28034

Waugh, D. W. and Hall, T. M.: Age of stratospheric air: theory, observations, and models, *Rev. Geophys.*, 40, 1010, doi:10.1029/2000RG000101, 2002. 28015, 28016, 28022, 28023, 28028

5 Waugh, D. W., Plumb, R. A., Elkins, J. W., Fahey, D. W., Boering, K. A., Dutton, G. S., Volk, C. M., Keim, E., Gao, R.-S., Daube, B. C., Wofsy, S. C., Loewenstein, M., Podolske, J. R., Chan, K. R., Proffitt, M. H., Kelly, K. K., Newman, P. A., and Lait, L. R.: Mixing of polar vortex air into middle latitudes as revealed by tracer–tracer scatterplots, *J. Geophys. Res.*, 102, 13119–13134, 1997. 28024

Observed temporal evolution of global age of air

G. P. Stiller et al.

Title Page

Abstract

Introduction

Conclusions

References

Tables

Figures

◀

▶

◀

▶

Back

Close

Full Screen / Esc

Printer-friendly Version

Interactive Discussion



Observed temporal evolution of global age of air

G. P. Stiller et al.

Table 1. “Over-aging” of non-tropical air due to in-mixing of mesospheric, SF₆-depleted air.

Event	Δage of vortex air (yr)	Amount of vortex air (mole)	“Over-aging” of non-tropical air (yr)
SH2002	0.50	0.23×10^{17}	0.008
NH2003	0.50	0.14×10^{17}	0.003
SH2003	1.00	0.94×10^{17}	0.071
NH2006	1.00	0.15×10^{18}	0.142
SH2006	1.50	0.15×10^{18}	0.188
NH2007	1.00	0.92×10^{17}	0.046
SH2007	3.00	0.12×10^{18}	0.183
NH2008	1.00	0.51×10^{17}	0.032
SH2008	2.00	0.86×10^{17}	0.083
NH2009	2.00	0.12×10^{18}	0.190
SH2009	4.00	0.10×10^{18}	0.207

[Title Page](#)
[Abstract](#)
[Introduction](#)
[Conclusions](#)
[References](#)
[Tables](#)
[Figures](#)
[Back](#)
[Close](#)
[Full Screen / Esc](#)
[Printer-friendly Version](#)
[Interactive Discussion](#)


Observed temporal evolution of global age of air

G. P. Stiller et al.

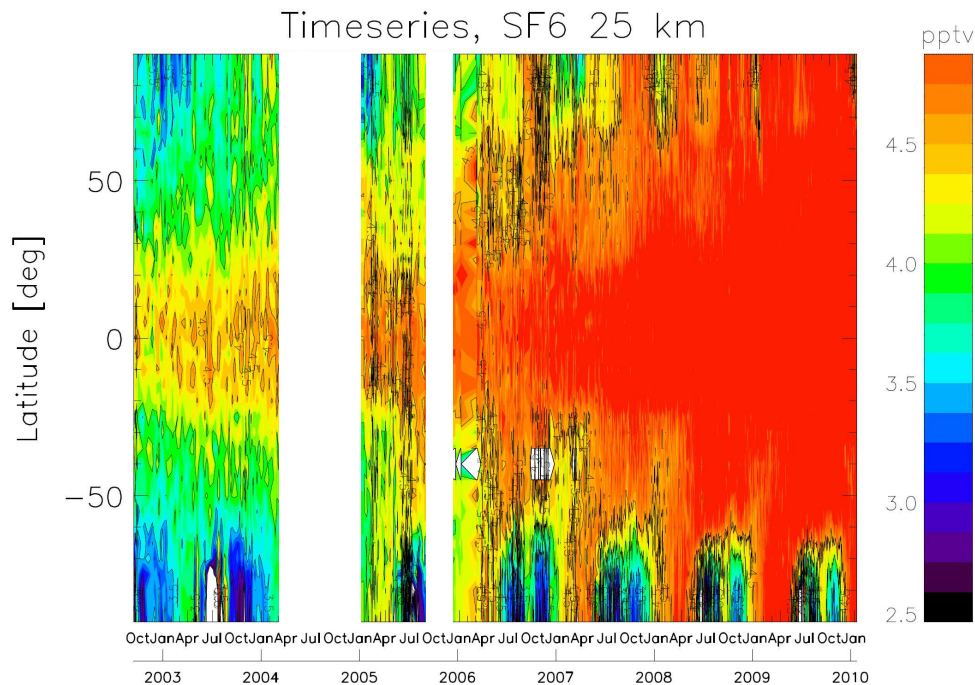


Fig. 1. Time series of SF₆ volume mixing ratio over all latitudes at 25 km altitude for the period September 2002 to January 2010. The white bars indicate data gaps where no measurements were available.

Title Page

Abstract

Introduction

Conclusions

References

Tables

Figures

◀

▶

◀

▶

Back

Close

Full Screen / Esc

Printer-friendly Version

Interactive Discussion



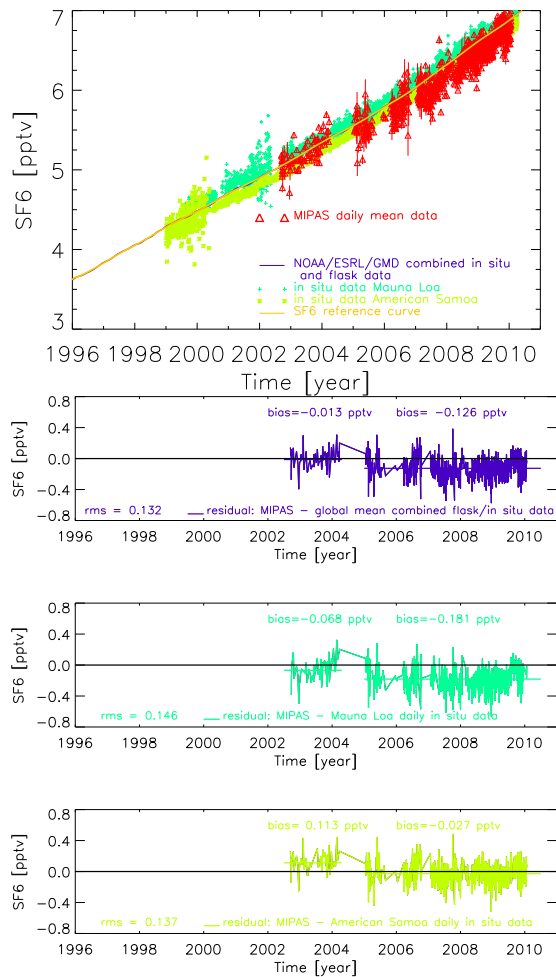


Fig. 2. Caption on next page.

Observed temporal evolution of global age of air

G. P. Stiller et al.

Title Page

Abstract Introduction

Conclusions References

Tables Figures

◀ ▶

◀ ▶

Back Close

Full Screen / Esc

Printer-friendly Version

Interactive Discussion



Observed temporal evolution of global age of air

G. P. Stiller et al.

Fig. 2. Top panel: Tropical upper tropospheric time series of SF₆ from MIPAS observations (daily zonal averages between 17.5° S and 17.5° N and 9 to 15 km altitude; red triangles) together with monthly global mean combined flask and in situ data (violet line, hard to see), Mauna Loa Observatory daily mean in situ observations (dark green crosses), and American Samoa daily mean in situ observations (light green asterisks). The solid orange curve presents the SF₆ tropical reference curve derived as described in the text. Bottom panel: Daily mean deviations between MIPAS tropical upper tropospheric SF₆ volume mixing ratios and the monthly global mean combined flask and in situ data set (top), Mauna Loa Observatory daily mean in situ observations (middle), and American Samoa daily mean in situ observations (bottom). Numbers in the panels provide the rms over the whole MIPAS observation period, and the mean bias between MIPAS SF₆ vmr and the respective flask and/or in situ observations for the periods 2002 to 2004 and 2005 to 2010, respectively.

Title Page

Abstract

Introduction

Conclusions

References

Tables

Figures

⏪

⏩

◀

▶

Back

Close

Full Screen / Esc

Printer-friendly Version

Interactive Discussion



Observed temporal evolution of global age of air

G. P. Stiller et al.

Title Page

Abstract

Introduction

Conclusions

References

Tables

Figures

◀

▶

◀

▶

Back

Close

Full Screen / Esc

Printer-friendly Version

Interactive Discussion

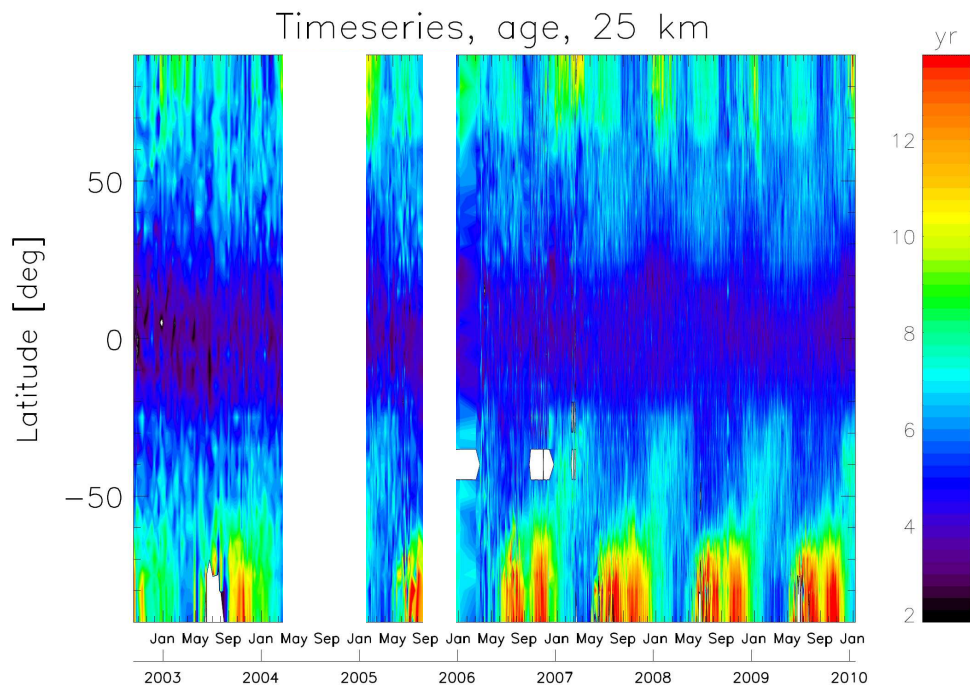


Fig. 3. Latitude-time cross-section of mean age of air at 25 km altitude for the period September 2002 to January 2010. White areas represent regions where no data are available.

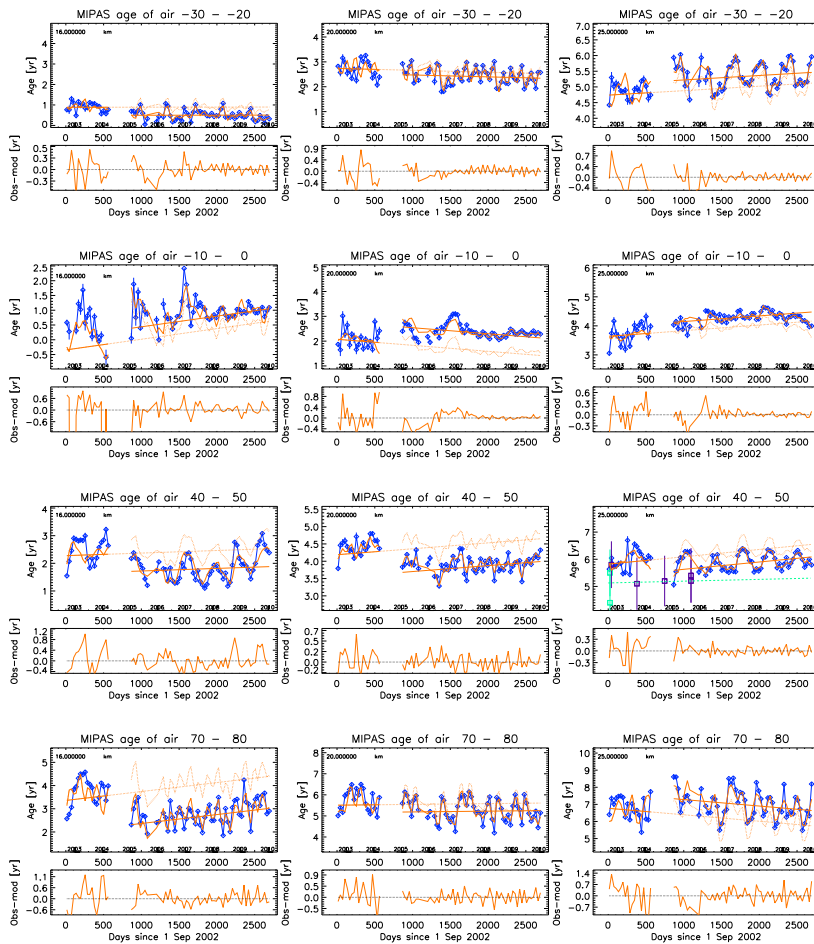


Fig. 4. Caption on next page.

Observed temporal evolution of global age of air

G. P. Stiller et al.

Title Page

Abstract Introduction

Conclusions References

Tables Figures

◀ ▶

◀ ▶

Back Close

Full Screen / Esc

Printer-friendly Version

Interactive Discussion



Observed temporal evolution of global age of air

G. P. Stiller et al.

Fig. 4. Temporal evolution of age of air for the Southern subtropics (30° S to 20° S) (top row), inner tropics (10° S to 0) (second row), Northern mid-latitudes (40° N to 50° N) (third row), and Northern polar region (70° N to 80° N) (bottom row) at 3 different altitudes (16 km, 20 km, 25 km). In the upper part of each panel, dark blue diamonds with error bars (the latter are often smaller than the diamonds and hardly visible) are the observed AoA monthly means and their SEM. The bold solid orange curve is the fit through the monthly mean data. The linear part of the regression is given as straight line. The dotted orange curve and straight line is the model without residual bias correction. In the panel for Northern mid-latitudes, 25 km, the 30-yr AoA trend as derived by Engel et al. (2009) is included as a green dashed line, together with the data points and their uncertainties of the Engel et al. (2009) study which fall into the observation interval of MIPAS (green and violet squares, color coding of latitudes adapted to the original figure). In the lower part of each panel, the residuals between observed monthly mean AoA and the model are shown.

[Title Page](#)[Abstract](#)[Introduction](#)[Conclusions](#)[References](#)[Tables](#)[Figures](#)[◀](#)[▶](#)[◀](#)[▶](#)[Back](#)[Close](#)[Full Screen / Esc](#)[Printer-friendly Version](#)[Interactive Discussion](#)

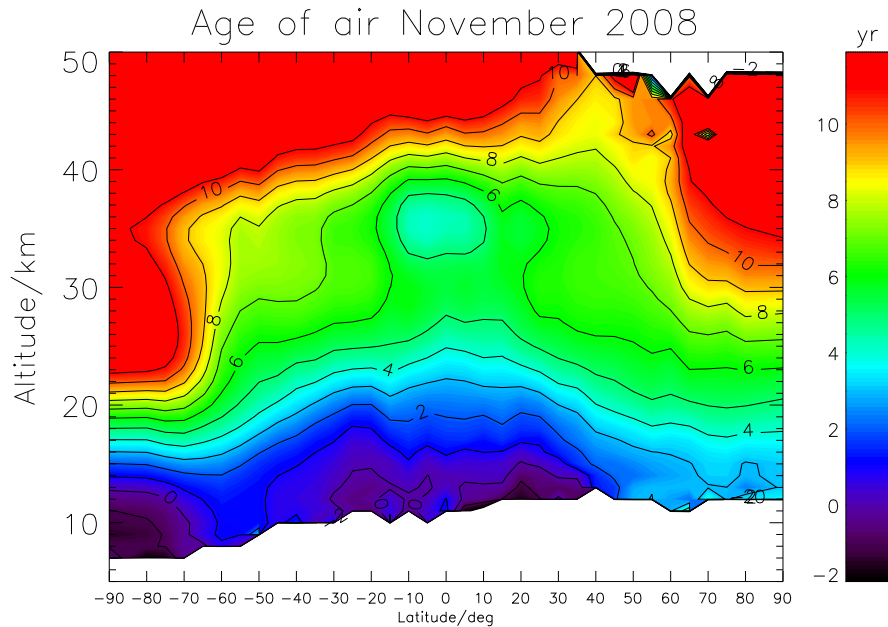


Fig. 5. Zonal mean distribution of mean age of air of November 2008 showing the beginning break-down of the polar vortex and the intrusion of relatively young air to polar latitudes around 35 km.

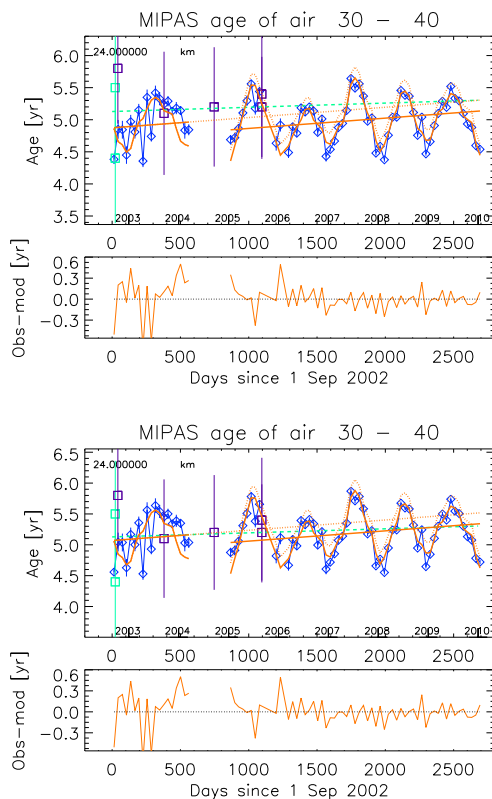


Fig. 6. Temporal evolution of mean age of air for 30° N to 40° N, 24 km with correction of "over-aging" (top) and without (bottom). The linear increase in the top panel is $(0.59 \pm 0.08) \text{ yr decade}^{-1}$, compared to $(0.61 \pm 0.08) \text{ yr decade}^{-1}$ without "over-aging"-correction. The green dashed line is the 30-yr trend derived by Engel et al. (2009), and the green and violet squares are the data points and their uncertainties of the Engel et al. (2009) study which fall into the observation period of MIPAS.

Observed temporal evolution of global age of air

G. P. Stiller et al.

Title Page

Abstract Introduction

Conclusions References

Tables Figures

◀ ▶

◀ ▶

Back Close

Full Screen / Esc

Printer-friendly Version

Interactive Discussion



Observed temporal evolution of global age of air

G. P. Stiller et al.

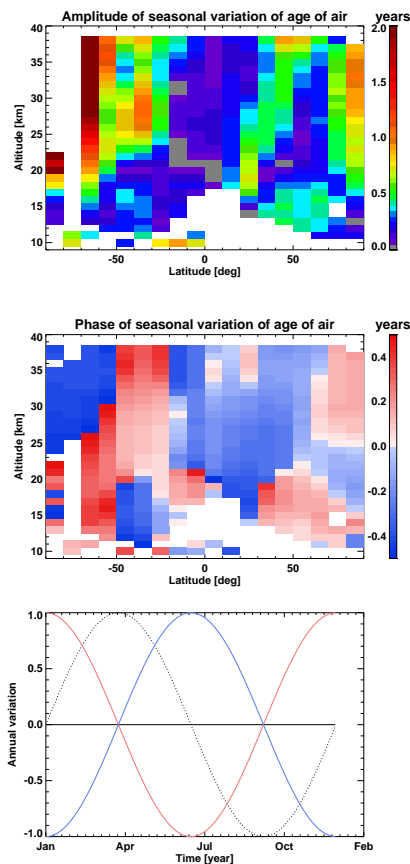


Fig. 7. Altitude-latitude cross-sections of amplitudes (top) and phases (middle) of the seasonal variation of mean age of air. The lower panel indicates how the phase shifts have to be read; example phase shifts shown are +0.25 yr (red) and -0.25 yr (blue).

[Title Page](#)[Abstract](#)[Introduction](#)[Conclusions](#)[References](#)[Tables](#)[Figures](#)[◀](#)[▶](#)[◀](#)[▶](#)[Back](#)[Close](#)[Full Screen / Esc](#)[Printer-friendly Version](#)[Interactive Discussion](#)

Observed temporal evolution of global age of air

G. P. Stiller et al.

Title Page

Abstract

Introduction

Conclusions

References

Tables

Figures

◀

▶

◀

▶

Back

Close

Full Screen / Esc

Printer-friendly Version

Interactive Discussion

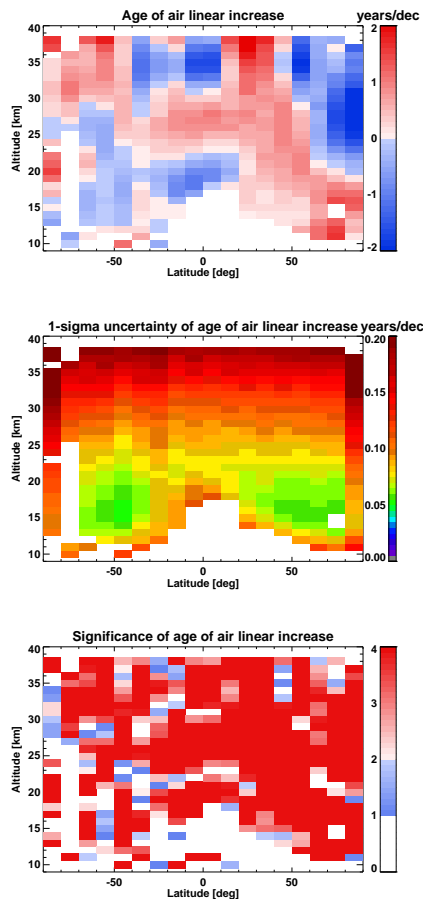


Fig. 8. Altitude-latitude cross-sections of the age of air linear increase/decrease over the years 2002 to 2010 (top), together with its 1- σ uncertainties (middle) and significance in terms of multiples of σ (bottom).

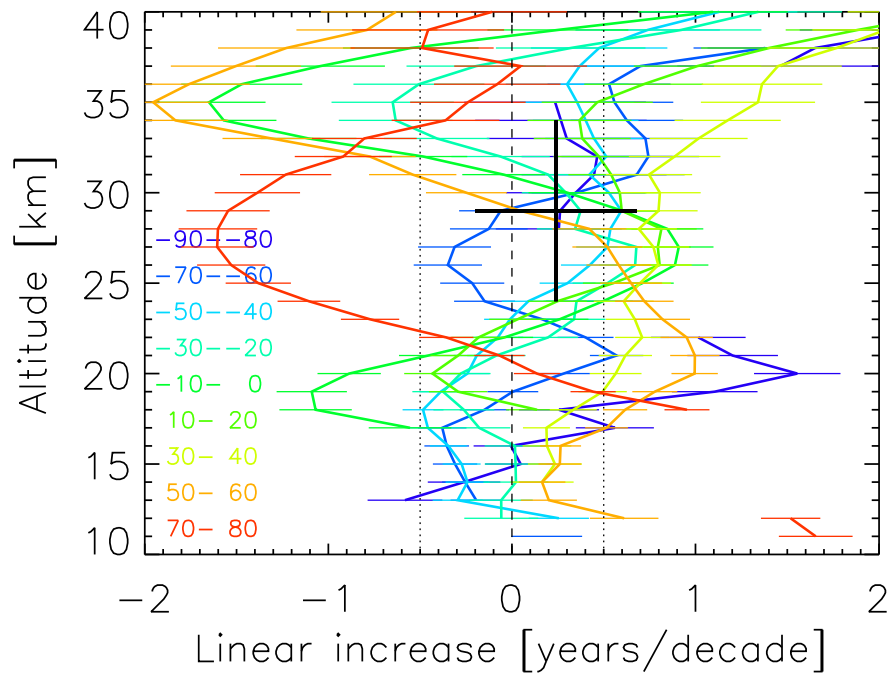


Fig. 9. Vertical profiles of the age of air linear increase/decrease over the years 2002 to 2010 for example latitudes. Horizontal bars give the $2\text{-}\sigma$ uncertainties of the linear variations. The 30-yr trend as derived by Engel et al. (2009) is also shown for comparison as a black cross indicating its valid altitude range and its $2\text{-}\sigma$ -uncertainty.

Observed temporal evolution of global age of air

G. P. Stiller et al.

Title Page

Abstract Introduction

Conclusions References

Tables Figures

◀ ▶

◀ ▶

Back Close

Full Screen / Esc

Printer-friendly Version

Interactive Discussion



Observed temporal evolution of global age of air

G. P. Stiller et al.

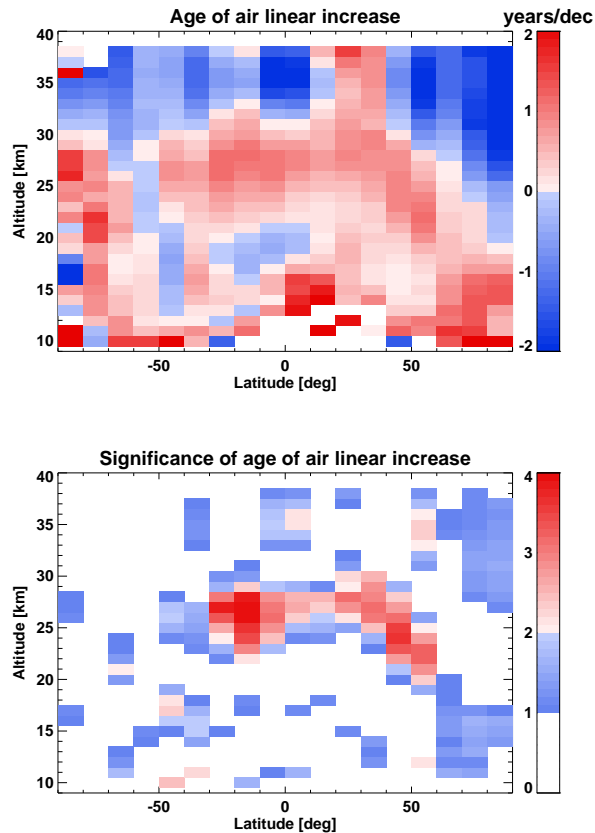


Fig. 10. Altitude-latitude cross-section of the AoA model-error corrected linear increase (top) and its significance in terms of multiples of σ (bottom) after including the model error and autocorrelations between the data points in the fit.

[Title Page](#)[Abstract](#)[Introduction](#)[Conclusions](#)[References](#)[Tables](#)[Figures](#)[⏪](#)[⏩](#)[◀](#)[▶](#)[Back](#)[Close](#)[Full Screen / Esc](#)[Printer-friendly Version](#)[Interactive Discussion](#)